Fluorescent Imaging During Photodynamic Therapy of Skin Cancer

Master's Thesis
by
Tran Thi Thu Tam

April 2007

Abstract

Skin cancer is the most common of all cancers. Early detection and cure of skin cancer are very important to mankind. The possibilities of combination of powerful cancer imagery, fluorescence imaging and interactive treatment modalities based on photodynamic therapy (PDT) have potential to provide diagnostic capability and a promising treatment for many types of skin cancers.

The region- of- interest (ROI)/tumor is moving and deminishing during fluorescence imaging and PDT treatment. In this thesis, the abilities of using the tranparent template/mask as a mean of tumor marking are discussed. The development of an evaluated program which can be able to find the template marks and extract the ROI is also presented. Finally, the experimental results and the present status of clinical evaluation and future direction are discussed.

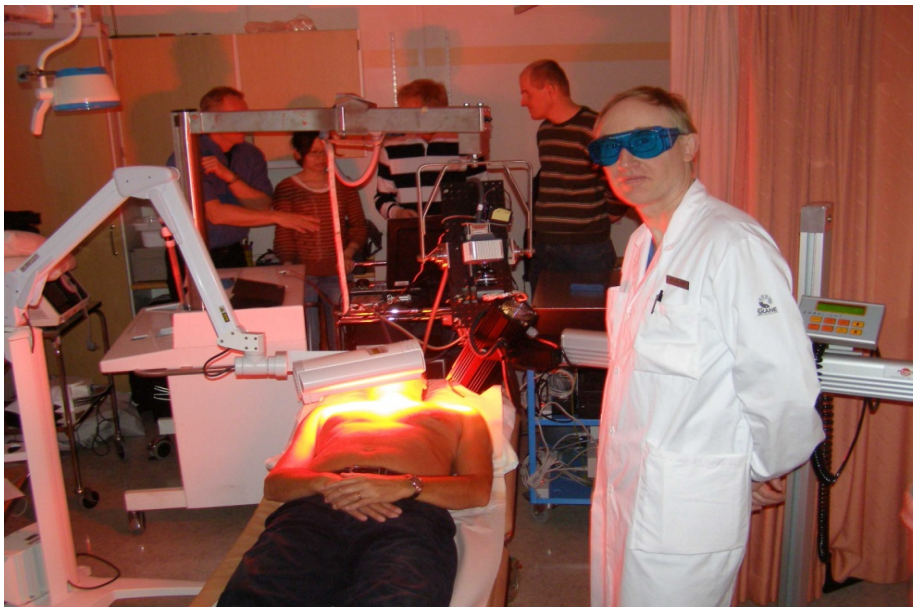

Figure 1: The picture of fluorescence imaging on patient on clinic at Lund University Hospital.

Contents

Chapter 1

Introduction

1.1 Background

Did you know that skin cancer is the most common of all cancers? The answer is yes. Skin cancer can occur anywhere on the body, but it is common in skin that has been exposed to sunlight, such as the face, neck, hands, and arms. The three most common types of skin cancer are Basal Cell Carcinoma (BCC), Squamous Cell Carcinoma (SCC) and Melanoma.

There is good news though, skin cancer can be cured if caught early. The first step in catching skin cancer is learning what it is and how to identify it. Fluorecence Imaging and Photodynamic Therapy (PDT) have become an interesting alternative to conventional therapy of skin cancer. Photodynamic therapy is based on the administration of a photosensitizing compound (photosensitizer) with its following activation by visible or near-infrared light. The resulting photodamages originate from the production of singlet oxygen and other reactive oxygen species. These react with cellular targets leading to damage of the biological tissue. Fluorescence imaging techniques are based on the detection of fluorescence of endogenous species, such as collagen and nicotinamide adenine dinucleotide, which contribute partly to broadband autofluorescence in the blue/green spectral region, or the fluorescence of exogenous photosensitizers or their precusors. The photosensitizers are fluorescent and have been shown to accumulate preferentially in many types of cancer in comparison with the surrounding healthy tissue [21]. This phenomenon is the foundation on which photodynamic therapy (PDT) is based on.

A multispectral fluorescent imaging system has been developed at Lund University Medical Laser Center. The system has been used in Lund University Hospital in diagnostic applications before, during and after photodynamic therapy of skin lesions on patients.

1.2 Goal of diploma work

The tasks of the present Master's thesis are:

1. To handle the multispectral fluorescence imaging system.
2. To develope a part of the evaluation program that provides the posibility to automatically follow the image patern in several sequentially acquired images.
3. To investigate fluorescence before, during, and after photodynamic therapy treatment.

1.3 Outline

The organization of this diploma work is as follows. It starts with Chapter 2, an overview of properties of light and the theory of light propagation in tissue. Then, in Chapter 3 some basic characteristic features of the most common skin cancers are given. The theories of photodynamic therapy (PDT) and fluorescence diagnostics are described in Chapter 4. The development of a program for image tracking is in Chapter 5. The results are shown in Chapter 6. The discussions are in Chapter 7. The conclusions are in Chapter 8. Finally, the suggestions for the future tasks are in Chapter 9.

Chapter 2

The interaction of light with tissue

In this chapter an overview of the general properties of light, and the description of tissue-light interactions are given.

2.1 Light

Light is dualistic in nature. It can be described as an electromagnetic wave or as a package or quantum of energy - a photon. The electromagnetic spectrum ranges from radio waves through infrared and visible light to X-rays and gamma radiation. The wavelength, λ, or the frequency, υ, are used to describe the radiation when the wave nature is considered, and the energy, E, is used when light is regarded as a stream of photons. The relation between these quantities is described as follows.

$$E = h\upsilon = h\frac{c}{\lambda}[J] \tag{2.1}$$

$$c = \lambda\upsilon[m/s] \tag{2.2}$$

The spectrum of electromagnetic radiation is shown in figure 2.1.

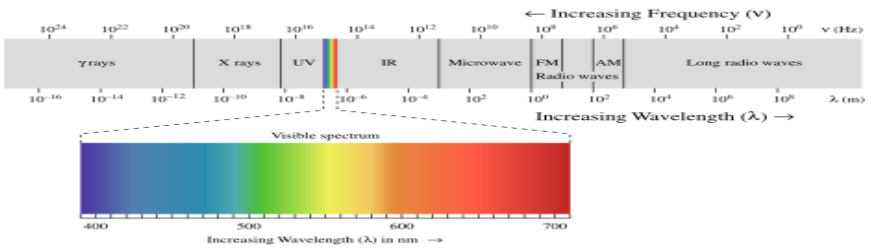

Figure 2.1: The spectrum of electromagnetic radiation.

2.2 Light propagation in tissue

When tissue is illuminated with light, several processes can occur, namely reflection, absorption, scattering, transmittance and fluorescence depending on the structure and geometry of the tissue, and its constituents. In this section, these optical phenomena are described in detail. Fluorescence process will be described in more detail in Chapter 5.

2.2.1 Absorption

Absorption of light can take place inside the tissue. If an incoming photon carries energy that matches the gap between two energy levels in a molecule, it can be absorbed. The absorption in tissue is described by the absorption coefficient, μ_a, which is defined as the probability of absorption per unit length and is expressed in the unit $[m^{-1}]$. The absorption coefficient in tissue is the sum of the absorption coefficients for the present absorbers, or chromophores. The absorption coefficient in tissue is strongly wavelength dependent. In figure 2.2 the absorption as a function of wavelength for different tissue chromophores is shown. Haemoglobin is a pigment that carry oxygen in the red blood cells, and melanin is a pigment in skin, hair, and in the iris of the eyes. They absorb strongly in the blue and UV regions. Water absorbs in the UV and IR regions.

As can be seen, in the wavelength region between 650 - 1300 nm, the total absorbance is lowest in tissue. This region is often called the *tissue optical window*. Light can penetrate further into the tissue when the absorption is low. Hence this region is favorable to use for tissue diagnostics.

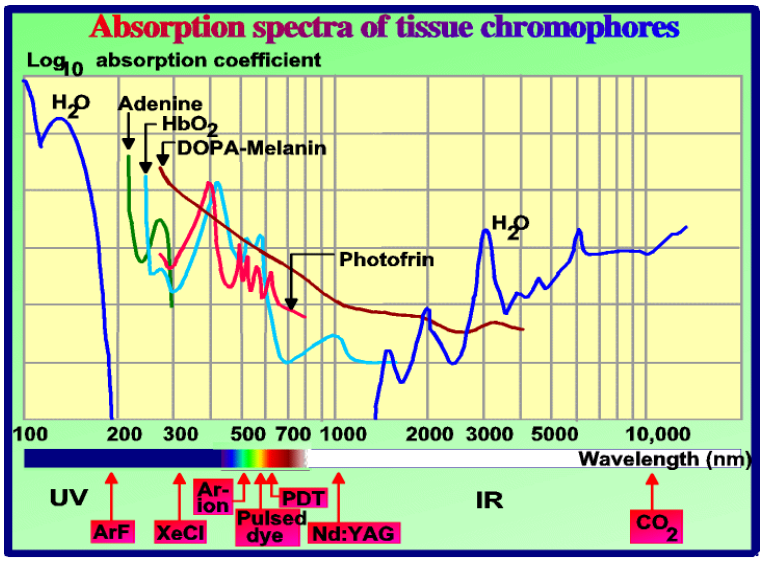

Figure 2.2: The absorption spectra of tissue chromophores [10].

2.2.2 Reflection, Scattering, Transmittance

When a light source illuminates tissue, a certain percentage of the photon beam that impinges onto the tissue surface, can be reflected at the surface due to differences in refraction index between air and tissue. Only part of the light that is transported into the tissue, will be transmitted.

Light interacts with the different structures inside the tissue which will cause the light to be scattered. The scattering coefficient, μ_s, which is defined as the probability of scattering per unit length and is expressed in unit $[m^{-1}]$. The scattering coefficient shows a dependence on wavelength, but it is only a small decrease as the wavelength is increased [1].

Scattering in tissue is not isotropic, the light is mostly scattered in the forward direction. The scattering direction is described by the scattering anisotropy or g-factor, which is related to the average scattering angle by the relation below:

$$g = \langle cos\theta \rangle \tag{2.3}$$

Where θ is the angle between the incoming photon trajectory and the scattered photon trajectory. The factor g is in the range of 0.7-0.98 in different tissue types [1]. If light is scattered many times in tissue, the light will become diffuse and the g-factor and μ_s cannot be separated. The reduced scattering coefficient, $\mu_s^{'}$ is introduced. It is described as follow:

$$\mu_s^{'} = \mu_s(1 - g). \tag{2.4}$$

The reduced scattering coefficient is very useful in tissue optics, since many methods, which measure tissue optical parameteres, only measure the reduced scattering coefficient.

2.3 Effect of ultraviolet light (UV) on the skin

The wavelength range of ultraviolet radiation (UVR) is between 280 nm and 400 nm. It is divided into three regions, namely, 200-280 nm (UVC), 280-320 nm (UVB), and 320-400 nm (UVA). Sunlight has a profound effect on the skin causing skin cancer, and a host of skin changes. Exposure to UV light, UVA, UVB, from sunlight accounts for 90 % of the symptoms of premature skin aging.

- UVC radiation is almost completely absorbed by the ozone layer and does not affect the skin [7].
- UVB radiation affects the outer layer of skin, the epidermis, and is the primary agent responsible for sunburns [7].
- UVA is a major contributor to skin damage. UVA penetrates deeper into the skin and works more efficiently [7].

Chapter 3

Skin cancer

Skin cancer is the uncontrolled growth of skin cells. If left unchecked, these cancer cells can spread from the skin into other tissues and organs [2].

In this chapter, the structure of skin and a brief overview of the basic characteristic features of skin cancers are given.

3.1 Incidence

Skin cancer is the most common and the most curable of all cancers. Worldwide, one out of three cancers is skin-related [3]. The occurrence of skin cancer is increasing in most countries through out the world [4]. According to the World Health Organization (WHO), skin cancer incidence is rising. By WHO estimates, 132 000 cases of malignant melanoma (66 000 deaths) and more than 2 million cases of other skin cancers occur annually [3]. The incidence of skin cancer is increasingly rapidly, primarily because of increased recreational exposure to ultraviolet (UV) light [5].

Skin cancer can occur anywhere on the body, but it is most common on skin that has been exposed to sunlight, such as the face, neck, head, hands, and arms.

3.2 The structure of skin

It is important to know the structure of the skin in order to understand the different kinds of skin cancer, as well as some mechanisms involved in PDT and fluorescent imaging. Figure 3.1 shows a schematic cross-section of skin. As can be seen, the skin is built up by three layers [4].

The epidermis layer is seen on the surface of the skin. It is made up of cells called keratinocytes, which are stacked on top of each other, forming different sub-layers [6]. The keratinocytes develop at the bottom and rise to the top, where they are shed from the surface as dead cells. This layer is constantly renewing itself, the live cells changing into dead, hard, flattened cells. Another type of cells in the epidermis is the melanocytes. These cells produce the melanin, which is the pigment that protects the skin from UV radiation. The amount of pigment in the skin depends mostly on genetic

properties and exposure to sunlight [4].

The second layer of the skin is dermis which consists of connective tissue and is much thicker than the epidermis. It is responsible for the skins pliability and mechanical resistance and is also involved in the regulation of the body temperature. The dermis supplies the avascular epidermis with nutrients by means of its vascular network. It contains sense organs for touch, pressure, pain and temperature, as well as blood vessels, nerve fibers, sebaceous and sweat glands and hair follicles [6].

The undermost layer, subcutaneous layer which is the layer below dermis consists of loose connective tissue and much fat. It acts as a protective cushion and helps to insulate the body by monitoring heat gain and heat loss [6].

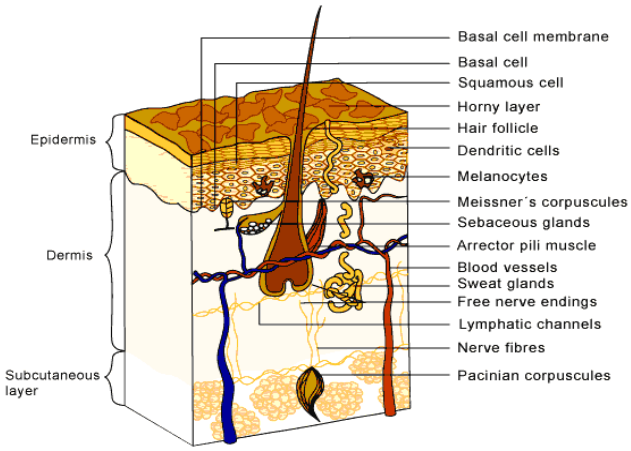

Figure 3.1: The structure of skin [6].

3.3 Types of skin cancer

There are three main types of skin cancer: Basal Cell Carcinoma (BCC), Squamous Cell Carcinoma (SCC), malignant melanoma [3].

The most common type of skin cancer is BCC which accounts for approximately 75 percent of all skin cancers [3]. It is estimated that in Sweden with a population of 9 million inhabitants approximately 25 000 people are diagnosed with one or more new BCC lesions each year [8]. This highly treatable cancer starts in the basal cell layer of the epidermis and grows very slowly. BCC usually appears as a small, shining bump or nodule on the skin-mainly those areas exposed to the sun, such as the head, neck, arms, hands, and face.

Another main type of skin cancer is SCC which accounts for about 20 percents of all skin cancer cases [3]. This kind of skin cancer is treatable. SCC may appear as nodules red, scaly patches of skin, and may be found on the face, ears, lips, and mouth. However, SCC can spread to other parts of the body.

Malignant melanoma is less common kind of skin cancers but it is the most deadly, accounting for 79 percent of all deaths related to skin cancer. Maglignant melanoma starts in the melanocytes-cells that produce pigment in the skin. Malignant melanomas usually begin as a mole that turns cancerous. This cancer may spread quickly. This type of skin cancer is dangerous because the melanin content in malignant melanoma is so high that this type of tumor is not suitable for either PDT or fluorescent diagnosis [4].

Chapter 4

Photodynamic Therapy (PDT) and Fluorescence Diagnostics

In this chapter, the short history of PDT and fluorescence diagnostics is introduced, furthermore, the theories of photodynamic therapy and fluorescence diagnostics are discussed.

4.1 History introduction

The use of light as a therapeutic agent can be traced back over thousands of years. It was used in ancient Egypt, Indian and China to treat skin diseases, such as psoriasis, vitiligo and cancer, as well as rickets and even psychosis [14, 15]. During the 19th century, phototherapy developed into a science, with the Danish physician Niels Finsen who described the successful treatment of smallpox using red light, which prevented suppuration of the pustules [16]. The first report of administration of photosensitizer in humans was in 1900 by Prime, a French neurologist, who used eosin orally in the treatment of epilepsy. He discovered that this induced dermatitis in sun-exposed areas of skin [16]. This discovery then led to the first medical application of an interaction between a fluorescent compound and light which Tappiener, the first scientist, to use PDT on patient. Today PDT is a clinically accepted method which is applied in several clinical situations.

The research on fluorescence imaging using exogenous tumor markers for tissue diagnostics and the developments of photodynamic therapy of malignant lesions with fluorescent photosensitizers are tightly connected [9]. The photosensitizer, for example, haematoporphyrin deriative (HpD) which was used in PDT, was also used as a fluorescent tumor marker for cancer diagnostics [26]. The second generation photosensitizers were developed, with improved properties. The introduction of 5-aminolevulinic acid (ALA) was applied for diagnostics of malignant tumors [26]. To avoid side effect, diagnostics based on only tissue autofluorescence became increasingly interest. The developments of instruments allowing quantitive detection schemes of the fluorescence are considered. A number of fluorescence detections have developed for a variety of clinic applications, using different algorithms to distinguish maglignant from normal tissue.

4.2 Photodynamic Therapy (PDT)

The treatment of malignancies based on photoinduced reactions involving oxygen is called Photodynamic Therapy, PDT (earlier it was called Photoradiation Therapy, PRT) [13] . The main advantages of PDT are sensitivity, nice healing and the ability to treat the same area several times, if necessary. The main disadvantage of PDT is the limited light penetration, which can be improved by development of new photosensitizes, and using the concept of interstitial PDT.

4.2.1 PDT treatment

PDT is a promising treatment for cancer and other nonmalignant conditions, which involves the administration of a photosensitizing agent followed by exposure of the tissue to visible non-thermal light (400-760 nm). When the photosensitizer is illuminated with light of the appropriate wavelength, the molecule is excited. This produces a series of molecule energy transfers leading to the liberation of singlet oxygen, a highly reactive and cytotoxic species. This singlet oxygen reacts with molecules in the tissue, resulting in cell death. Photosensitizers are often taken up by malignant or dysplastic tissue with some selectivity, and light delivery can be targeted to the appropriate tissue. The combination of drug uptake in malignant tissues and selective light delivery has the potential to provide a tumor with efficient cytotoxicity and limited damage to the surrounding normal tissue [16].

Here are steps of treatment, see also figure 4.1 [17, 18]:

1. A light-sensitive drug (PS) is injected intravenously into the patient.
2. The PS is retained by malignant tissue, remaining inactive until exposed to a specific wavelength of laser light.
3. Laser energy is delivered directly to the cancer site through a flexible fiber optic device and manipulated by the physician.
4. When the drug is activated by the energy of laser light, it will create a toxic form of oxygen that destroys the cancerous cells with minimal damage to surrounding healthy cells. The treated area shows evidence of swelling, infiltration of inflammatory cells, and tissue breaks down within 24 hours.

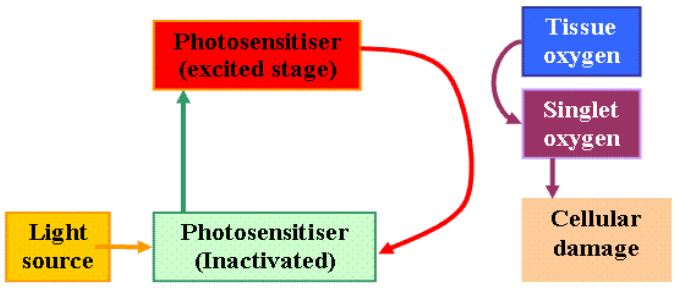

Figure 4.1: The scheme of the principle of PDT and photochemical reactions.

4.2.2 The photosensitizers (PS)

Photosensitizers are chemical substances or medications that increase the sensitivity of the skin, eye or others (more internal) organ usually not exposed to light to irradiation by optical radiation, usually to UV radiation. The term photosensitization covers all reactions in which a substance activated by light causes a biologic effect [11]. The most common photosensitizers also have fluorescing properties which can help for localization and characterization of various diseases. This allows convenient in vivo monitoring of the accumulation of the photosensitizer and the progress of the therapy. In the following, the photosensitizers with fluorescent properties will be concerned.

Some photosensitizers

Many kinds of compounds have been investigated in the search for the ideal photosensitizer for PDT. There are some basic properties that characterize an ideal photosensitizing compound. First of all, a high degree of selective accumulation of photosensitizer in malignant tissue is desirable, in order to only destroy the tumor tissue and low toxicity to a surrounding healthy tissue. Further, a high quantum yield for singlet oxygen generation is favorable for an efficient treatment. The research also requires finding the compounds which absorb far out in the red region, towards the borders of the infrared, where the penetration depth of the treatment light is at its maximum. A fast clearance rate of the photosensitizers is preferable to help saving the normal tissue, where the available photosensitizer concentration is low. Another important aspect is that the clearance times and the accumulation are short to minimize skin photosensitivity. A brief description of several photosensitizers is given as below:

Porphyrins

Pophyrins is a refined form of haematoporphyrin derivative (HpD), the first generation of photosensitizer. The basic structure of porphyrin consists of four pyrrole units linked by four methine bridges. Porphyrins have five peaks in the absorption spectrum, the strongest absorption peak at about 400 nm (the Soret band), and the weakest at about 630 nm. The fluorescence is characterized by a dual-peaked emission in the red wavelength region, at about 630 nm and 700 nm. Protoporphyrin IX is one of the most utilized photosensitizers [11].

Chlorins

Chlorins are reduced porphyrins. Chlorins have the strongest absorption peaks in the red part of the spectrum, which give the compound green colour. Benzoporphyrin derivative (BPD) is a chlorin, synthesized from protoporphyrin. It has strong absorption wavelength at 690 nm. It can accumulate rapidly in the tumour, allowing light irradiation the same day as injection. With skin photosensitization, it retains for a short time, less than a week.

mTHPC (Foscan)

Meso-tetrahydroxyl tetraphenyl chlorine (m-THPC) is effective at low drug and light doses. m-THPC-induced PDT can be used for deeper tumor destruction (up to approximately 1cm depth) and larger tumors can be effectively treated.

δ-aminolevulinic acid (ALA)

There are some second generation photosensitisers that have been investigated to improve the effectiveness of PDT such as 5-aminolaevulinic acid (5-ALA), which is the metabolic precursor of protoporphyrin IX (PpIX) in the biosynthetic pathway to haem, as be seen in figure 4.2 [12]. 5-ALA is not itself a photosensitizing agent. But after injection, 5-ALA metabolizes into PpIX, which can act as an endogenous sensitizer. PpIX has a broad band absorption spectrum centred on 400 nm, that induces a characteristic fluorescence, the dominant peak being at 635 nm. If this fluorescence can be detected from the cancerous lesions then it can be used routinely in cancer diagnostics. The advantages of using ALA-induced fluorescence are that it can be applied topically to skin and photosensitization is deminished within 24 hours. The rapid clearance from the body shows that ALA is a promising approach for PDT treatment [20, 21].

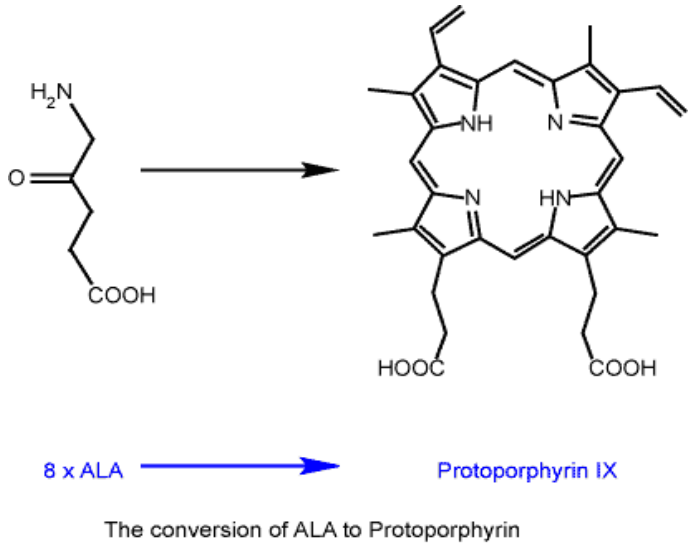

Figure 4.2: The conversion of ALA to PpIX in biosynthetic pathway [12].

Today, a large amount of new photosensitizers for PDT of various diseases is developed. Some examples are tin etiopurin, lutetium texaphyrin, tetra hydroxyphenyl chlorine, N-aspartyl chlorine.

Comparison of several different kinds of photosensitizers

Photosensitizers	Absorption wavelength	Medical indications	Properties of photosensitizers
Porphyrin Hematoporphyrin(Hp) Photofrin (Photogem,Photosun)	620 nm 630 nm	Esophageal cancer lung cancer bladder cancer brain cancer neck cancer	Long skin sensitivity
Benzoporphyrin (BDP-MA)	690 nm	Psoriasis	Short skin sensitivity, short time after injecting photosensitizers, the laser light is illuminated.
Lutetiumtexaphyrin (Lu-tex)	740 nm	Breast cancer Melanoma	Short skin sensitivity
Chlorin Chlorin e6(Npe6) Meso tetrahydroxyphenyl chlorine (m THPC, Foscan)	665 nm 650 nm skin cancer	Esophageal cancer Lung cancer Mouth cancer	Injection, non-sensitivity for the skin
5-Amino levulinic (ALA,Protoporphyrin IX)	630 nm	Skin cancer Bladder cancer	Short skin sensitivity

4.2.3 Photodynamic therapy dosimetry

The clinical efficacy of PDT treatment depends on a number of parameters such as tissue oxygenation status, photosensitizer (dose, tissue localization, kinetics, etc) and illumination (wavelength, light dose, fluence rate, photoproduct generation). Some of these factors are mentioned bellow.

Illumination

Light dosimetry [19]:

The total light dose is the total light energy density [J/cm^2] , delivered to the irradiated area. This is calculated as the product of irradiance, or fluence rate [W/cm^2] , and the treatment time[s]:

$$Totallightdose(J/cm^2) = fluencerate(W/cm^2) \times treatmenttime(sec) \quad (4.1)$$

Any red light at 635 nm can be used for the treatment. For ALA-PDT, a wide range of light doses has been implemented, ranging from 30 J/cm^2 to 540 J/cm^2. The general idea is that there are still photosensitizer molecules left when light is illuminated with

suitable light dose. The presence of photosensitizer molecules in superficial tissue can be investigated with fluorescence imaging measurements [11].

Fluence rate

To increase the treatment effect, the low fluence rates have been used. With high fluence rates, the oxygen is depleted fast and thereby stop the photochemical reaction. Mathematical simulations of the oxygen consumption, fluence rate of 50 mW/cm^2, estimates that cells remote enough from a capillary, may reside at oxygen levels low enough to avoid or minimise damage mediated by singlet oxygen [11].

In vivo photosensitizer dosimetry:

Photosensitizer concentration in tissue is an issue of significant interest. Recent in vivo studies have shown large variation of photosensitizer in different tissue types [23]. The fluorescence and measurements of photosensitizer can be made interstitially using optical fibers.

In vivo oxygen dosimetry :

Oxygen is one of the three key ingredients of PDT (photosensitizer, light, oxygen). An interesting consequence of this oxygen dependence is the effect of the fluence rate on PDT. The reduced efficiency of tumor destruction has been reported when the fluence rate in the ranges (100-200 mW/cm^2) were used. The reason of this lower effect has been attributed to oxygen depletion during the irradiation caused by oxygen consumption in the photochemical reaction [23] .

4.3 Fluorescent diagnostics

The basic theory of fluorescence,a brief description of tissue autofluorescence and fluorescence tumor markers are given in this chapter. Fluorescence detection techniques, namely point monitoring systems and imaging systems will be discussed in the last part of this chapter.

4.3.1 Fluorescence

An energy level diagram of molecules consists of many electronic energy levels. Molecules can rotate and vibrate, split the electronic energy levels into many other levels. At room temperature most molecules occupy the lowest vibrational level of the electronic ground state (S_0). When absorption of an incoming photon which has energy matches the energy difference between two levels of molecules, the molecules will be excited and go to either the first, (S_1) , or second (S_2) , excited state.

Once a molecule has absorbed energy, there are a number of ways by which it can return to the ground state. Different processes can be illustrated in a Jablonski diagram which is shown in figure 4.3. If the photon emission occurs between states of the same spin state (e.g.$S_1 \longrightarrow S_0$, this is termed *fluorescence*. A transition of the molecule into a triplet state is also possible. It takes a long time for the molecule to return to the

ground state because the transition from a triplet state to a single state is forbidden. This process is called *phosphorescence*. The lifetime of fluorescence states are very short (10^{-5} to 10^{-8} seconds) and phosphorescence somewhat longer (10^{-4} seconds to minutes or even hours) [24].

The eye is sensitive in very small region of the electromagnetic spectrum, which ranges from 400 nm (violet) to 700 nm (dark red. However, alot of information is available from other wavelength bands. Spectroscopic and imaging systems can utilize the information, largely extent the capability of the eye.

The fluorescence phenomenon can reveal properties invisible to the naked eye.

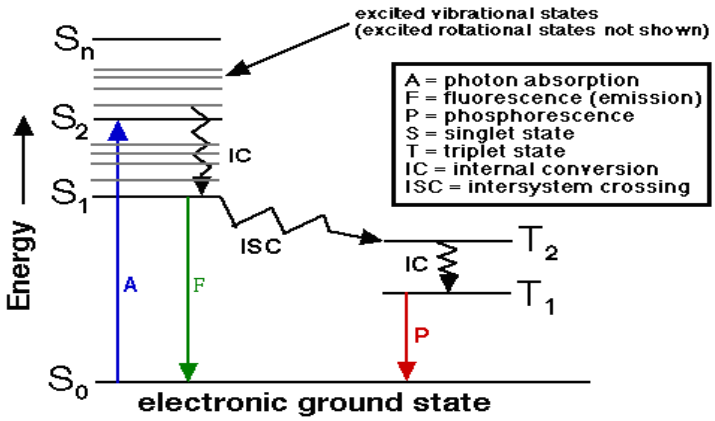

Figure 4.3: A Jablonski diagram where the different processes that can occur after excitation of the molecule are illustrated [24].

4.3.2 Autofluorescence and fluorescent tumor markers

Autofluorescence

Autofluorescence is the fluorescence which is obtained from different chromophores of tisue without presence of an external photosensitizer or other fluorescence markers [30]. The different chromophores of tissue emit fluorescence light in the blue-green wavelength region when they are exposed to UV or near UV light. The fluorophores can be e.g. nicotinamide adenine dinucleotide (NADH) and its phosphate (NADPH), tryptophan, elastin, collagen and porphyrins [1]. The wavelengths of the main excitation and emission peaks and the fluorescence life-times for the tissue fluorophores are shown in table 1 [25].

Fluorophore	λ_{exc}(nm)	λ_{em}(nm)	τ(ns)
Tryptophan	275	350	2.8, 1.5
Collagen	340 270 285	395 395 310	9.9, 5.0, 0.8
Elastin	460 360 425 260	520 410 490 410	6.7, 1.4, 8.2, 2.6, 0.5
Beta-caroten		520	9.6, 2.0, 0.3
NADH	350	460	0.6, 0.2
Endogenous porphyrins	400	610, 675	

Table 1: The wavelengths of the main excitation and emission peaks and the fluorescence life-times for the tissue fluorophores [25]

Most endogenous fluorophores are associated with the structural matrix of tissues or are involved in cellular metabolic processes. Tryptopphan is located in proteins in the mitochondria and dominates the autofluorescence when the excitation wavelength is shorter than 300 nm. Collagen and elastin are presented in, e.g., tendons and tissue stroma. The tissue fluorescence spectrum is dominated by collagen and elastin when excited with a nitrogen laser (337 nm). NADH is involved in cellular metabolism, dominates when the autofluorescence is excited at 365 nm [19].

The emitted autofluorescence for human tissue fluorophores after excitation with light of wavelength of 337 nm is shown in figure 4.4 [26].

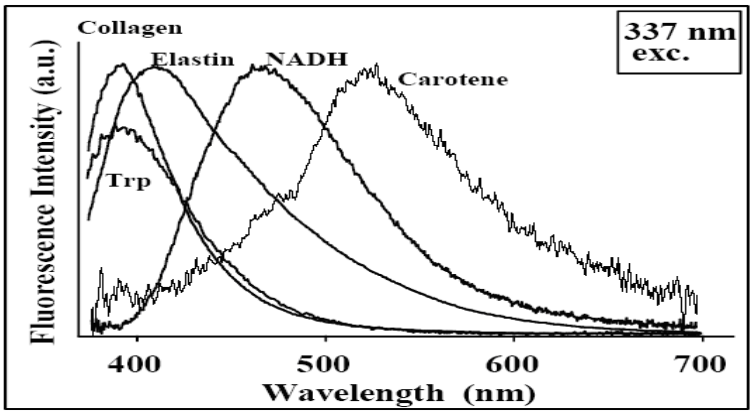

Figure 4.4: The emitted autofluorescence for human tissue fluorophores after excitation with light of wavelength of 337 nm [26] .

The autofluorescence is used for demarcation between normal and neoplastic tissue, for example breast tissue, cervix and skin cancer [4] because the autofluorescence is more intensive in normal tissue than in tumor tissue. The first reason is the blood flow in the tumor tissue increasingly. It can absorb a large amount of light and therefore not much fluorescence light is induced. Another reason is differences in concentration of certain molecules in tumors, changing the spectral finger print fluorescence [1].

Fluorescence tumor marker

The autofluorescence can change in different ways so it is difficult to diagnose a tumor by only studying the tissue autofluorescence. To increase the diagnostic potential of fluorescence diagnostics by adding fluorescent substances referred to as *fluorescent tumor marker* to the tissue. Fluorescent tumor markers are frequently selected to perform PDT, then called photosensitizers [4]. They have ability to accumulate to a higher degree in tumour tissues and hence an be applied for diagnostic purposes. Fluorescent tumor markers used in fluorescence diagnostics are chosen to provide a specific fluorescence in the red spectral region, where autofluorescence is weak so that it is easy to separate the fluorescence of the tumor marker from tissue autofluorescence.

δ-aminolevulinic acid (ALA)-induced protopophyrin IX (PpIX) is an example of a tumor marker, that is naturally occurring molecule in the body. PpIX has a dual-peaked fluorescence emission in the red spectral reagion, with one high and narrow peak at about 635 nm and one smaller and broader peak at about 705 nm. Therefore PpIX is found to be potential candidate for diagnostic purposes [31].

The characteristics of δ-aminolevulinic acid (ALA)-induced protopophyrin IX (PpIX) were mentioned more detail in photosensitizer section. It is compound used in the clinic work of this project.

4.3.3 Fluorescence detection techniques

The methods for fluorescence investigations are divided into two categories, *point-monitoring systems* and *imaging systems*. Using a point monitoring systems, the analysis of tissue fluorescence from a single position at the tissue surface, recorded as a fluorescence emission spectrum can be performed [11]. The advantages of these systems are that they give multispectral information and can be used for internal detections by means of optical fibers. The drawback is that only information from a small area is obtained, it makes time consuming when investigating a larger area. Due to this reason, many research on fluorescence imaging are developed. Both point monitoring and imaging systems can be used to record the intensity as a function of wavelength, or as a function of time, on a nanosecond time-scale [19].

Since the imaging system is the method which has been used in the major part of this project, only this technique is reviewed in more detail. Different types of fluorescence imaging instruments for diagnostic of malignancies are summarized below.

The first clinical bronchoscope using a mercury arc lamp source and an image intensified to amplify the faint fluorescence signal to a directly viewed image was presented in 1979. The drawback of this early system was that normal white light bronchoscopy could not be performed at the same time as the fluorescence examination [27].

Light-induced fluorescence endoscopy (LIFE) system has been developed commercially for endoscopic applications (Xillix Tech. Inc., BC, Canada). A continuous wave (CW) light source is used, emitting in the violet region. Using this system, tissue diagnostics is performed by evaluating the ratio between a red and a green autofluorescence emission band. The system has proved to give valuable diagnostic information when used in certain clinical specialties [6]. For example, this system have been used in de-

tection of cancers in the head and neck region [28, 29]. These systems are important because they can detect and localize tumours in early stage [1].

Another fluorescence imaging detection, a multi-color fluorescence imaging system, which can be utilized together with fibre-optical endoscopes, has been developed in Lund [11]. It is a more advanced system based on beam-splitting optics, providing four images of object, filtered at different emission bands. The four images can then be detected on an intensified CCD camera at the same time. The fluorescence was induced by means of pulsed ultraviolet light (390nm) from a frequency-doubled alexandrite laser. The excitation light was delivered by an optical fibre, and the fluorescence light was collected by a laryngoscope. Computer processing is used for viewing of the optimized contrast function image. The images were spectrally separated in three wavelength bands by means of dichroic mirrors. The following contrast function has been used for image processing.

$$F_c = (A - k_1 D)/k_2 B \tag{4.2}$$

Where A is sensitized-related fluorescence in the red region (580-750nm), B is autofluorescence evaluated in the blue region (420-480nm), D is an image in the green yellow region (480-580nm). The two constants, k_1 and k_2 , have different values for different applications, was used to produce images with optimized contrast between lesions and adjacent normal tissue. After image processing, a false-color image is shown on the computer screen, which delineats the tumorous tissue.

A multispectral fluorescence imaging system has been developed at Lund University Medical Laser Center. The system consists of a CCD-detector and a Liquid Crystal Tunable Filter (LCTF) providing the possibilities perform imaging in wavelength bands in visible spectral range. The system has been used in clinic prior, during and post photodynamic therapy of skin lesions on patients. This system is described in more detail in the experimental set-up section.

Chapter 5

Development of image tracking software for fluorescence imaging during photodynamic therapy

5.1 Aim

The first problem in fluorescence imaging is that the region-of-interest (RIO) to be imaged is moving during and between image acquisitions. This makes it time consuming and less accurate to evaluate and quantify the images. Thus there is a need for image processing software that finds the same tissue area in each image, see figures 5.1 below.

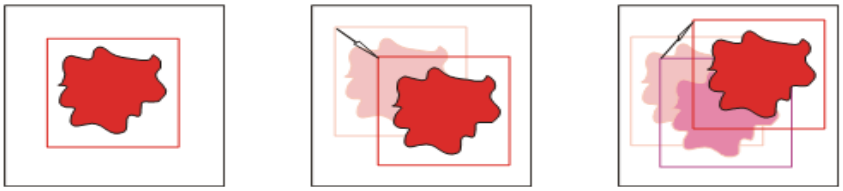

Figure 5.1: The schematic image where the ROI has moved. The red square is the ROI to be extracted.

The second problem is that the ROI is not constant in shape due to the imaged fluorescence which is consumed during the acquisition/treatment. To solve this problem the purpose of making a plastic mask to delineate the ROI. The scheme illustration is shown in figures 5.2 below.

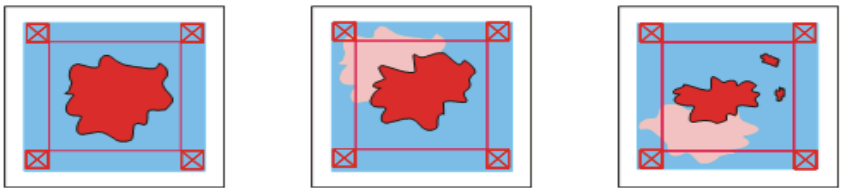

Figure 5.2: The illustration of transparent mask with marks (x) delineating the ROI. Here the imaged area is changing over time both in position and in size.

5.2 Implementation of solving the problems

1. Learn how to operate the multispectral fluorescence imaging system.
2. Constructing a template/mask.
3. Write a program that can extract the ROI.

5.3 Matlab program

The Matlab program was written. The features of this program are:

1. Ability to find the template marks automatically in each image.
2. Ability to extract automatically the same marks in each images, irrespective if these have moved.
3. Ability to extract a subimage, containing the ROI.

5.4 Mask design

Some kinds of mask were constructed of transparent paper with different marks. The marks were drawn with different colour pens, and different shapes (+, o, x, etc...).

Images were acquired in several wavelength bands to decide which one of the masks is the best. The mask with the red marks, x-shape, is the best because the marks are visible in several different wavelengths.

5.5 The set-up

The multispectral imaging system used for measurements are shown in figure 5.3.

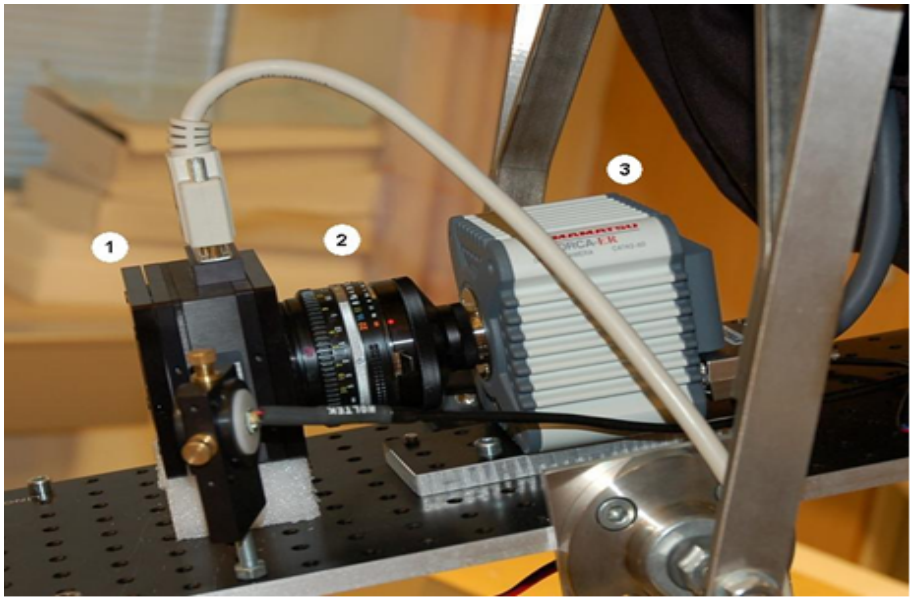

Figure 5.3: The fluorescence imaging system.

Excitation light source

Since the multispectral imaging system used to study emitted fluorescence in combination with photodynamic therapy, the light sources should be lasers.

The laser used in the experiment to illuminate to the sample that has wavelength of 375 nm.

On the clinic, the laser light was blue laser. It was developed at Riso National labratory, Denmark. The charateristics of this blue laser are as follow.

- 18mm PPKTP crystal
- Waistsize: 80m x 60m
- 51.8mm ROC for both mirrors
- Optical Length: 225mm
- FSR = 1.3GHz and Finesse = 30
- Roundtrip losses = 20 %
- Accept Bandwidth = 44 MHz

- 130mW blue output power with 286mW coupled to cavity
- 45 % power conversion efficiency.

The scheme of generate blue laser is shown in figure 5.4.

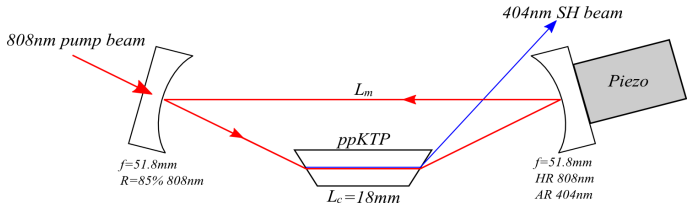

Figure 5.4: The scheme of generate blue laser.

Detector

The CCD-camera (HAMAMATSU C4742-80-12AG) provides images of the spectrally filtered object with an image size of 1344 pixels x 1024 pixels.

A liquid crystal tunable filter (LCTF)

A liquid crystal tunable filter (LCTF) provides the possibility to filter the incoming light so that spectrally resolved images can be acquired. This filter can filter wavelengths within the range 400 to 720 nm, with a spectral bandwidth of 20 nm.

A camera objective lens

The objective lens is placed in front of the LCTF to be able to change the field of view of the imaging system.

The sample

The piece of wood was chosen as a sample.
Fluorescent target has a round shape. It was made by an orange colour pen.
The mask was taped on the wood to mark the region-of-interest (the fluorescent target).
A ruler was taped on the wood to see the movements in the images.

Measurement equipment

A ruler which has a mm-scale, was used to measure the movements of the sample.

5.6 Experiment tests

5.6.1 xy-translated sample

The sample was moved 2-, 4-, 6 mm to the left and to the right in x-direction. The images of the sample were taken at each position.

5.6.2 The random movement of the sample

The images were taken while the sample was being moved randomly.

5.6.3 Clinical investigation of fluorescence imaging during photodynamic therapy

The patient had two skin tumors, one tumor was in his shoulder, one tumor was in his breast. The doctor put fluorescence tumor marker δ-aminolevulinic acid (ALA) on the tumors. The patient had to wait four hours so that ALA can be retained by malignant tissue. The constructed masks were covered in these two tumors. Then, the fluorescence imaging was taken. Afterthat, the photodynamic treatment was performed.

Chapter 6

Results

6.1 Experiment tests

6.1.1 xy-translated sample

The center image (when the sample was not moved) was taken with the light source, 375 nm, at the wavelength of spectral band of 630 nm. It was defined as the mask. The image results for the image of the mask is shown in figure 6.1.

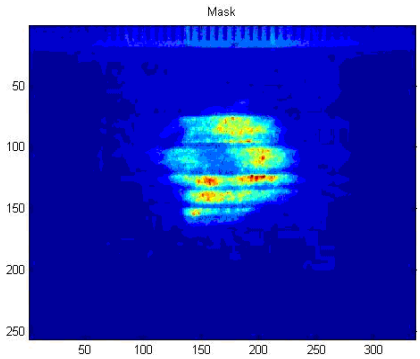

Figure 6.1: The image of the mask .

The Matlab program algorithm:

1. Choose the fours marks on the mask.
2. Program delete everything between the marks in the center.
3. Program convolutes the mask from 2) and all images at different times. Then the maximum for each image was found.
4. Calculate the computed movements of four marks (in pixels).

As can be seen in figures 6.2, the program can find four marks (in green colour) on the mask to mark ROI.

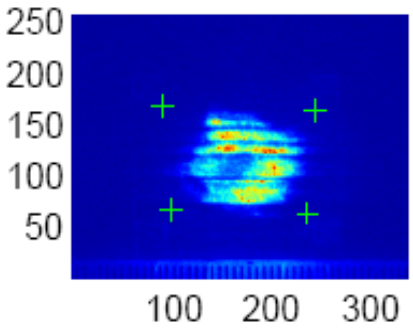

Figure 6.2: The image of the mask with four crosses.

The program can follow ROI and find four marks on the mask even if the sample has moved. As can be seen in figures 6.3, 6.4, 6.5, 6.6, 6.7 and 6.8, four marks which mark ROI (in red colour) are found when the sample moves 2-, 4- and 6 mm to the left and to the right.

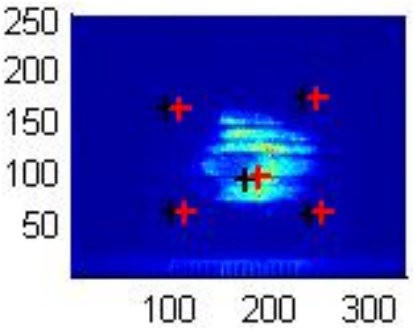

Figure 6.3: The image when the sample moves 2 mm to the left.

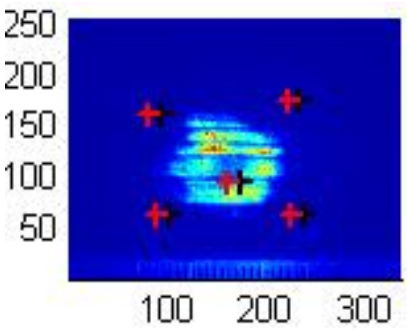

Figure 6.4: The image when the sample moves 2 mm to the right.

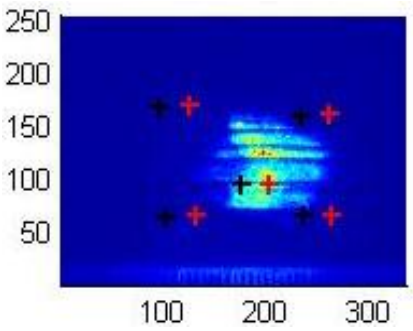

Figure 6.5: The image when the sample moves 4 mm to the left.

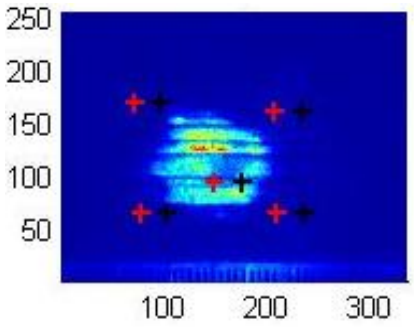

Figure 6.6: The image when the sample moves 4 mm to the right.

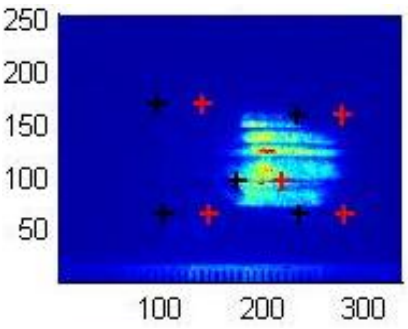

Figure 6.7: The image when the sample moves 6 mm to the left.

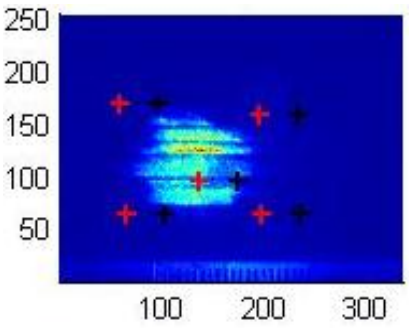

Figure 6.8: The image when the sample moves 6 mm to the right.

One of four marks in each image was followed when the sample moved 2- , 4- and 6 mm to the left and to the right. The illustration of these movements is shown as different colour points in figure 6.9. It can tell how much the computed movements are when the sample has moved 2, 4- and 6 mm to the left and to the right.

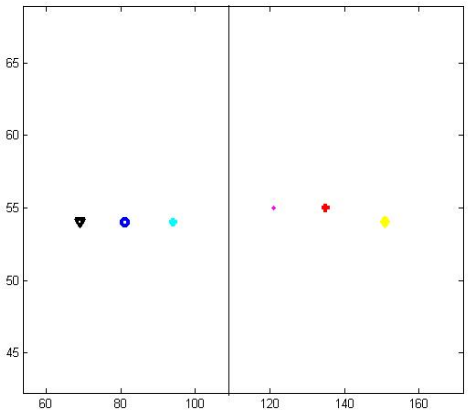

Figure 6.9: The illustration of the marks movement when the sample moved 2, -4, -6 mm to the left and to the right. Black: 6 mm to the right, blue: 4 mm to the right, green: 2 mm to the right, purple: 2 mm to the left, red: 4 mm to the left, yellow: 6 mm to the left.

The program can extract subimages which contain the same ROI (as can be seen in figures 6.10, 6.11, 6.12, 6.13, 6.14 and 6.15) even if the sample has moved 2-, 4-, 6 mm to the left and to the right.

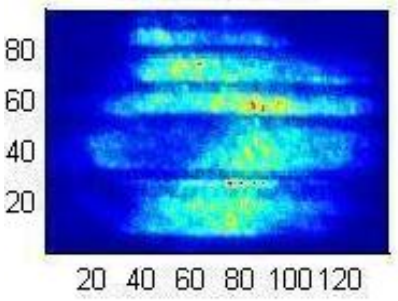

Figure 6.10: The subimage contains ROI when the sample moves 2 mm to the left.

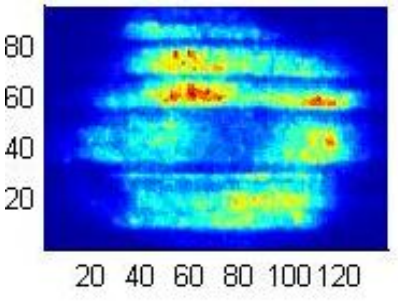

Figure 6.11: The subimage contains ROI when the sample moves 2 mm to the right.

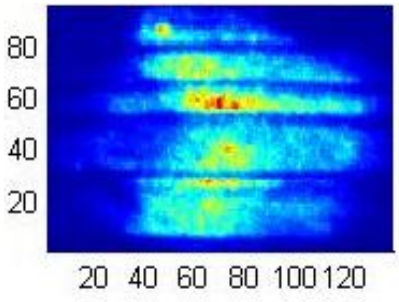

Figure 6.12: The subimage contains ROI when the sample moves 4 mm to the left.

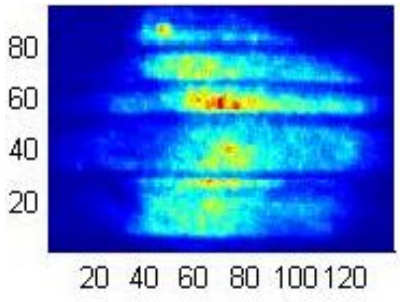

Figure 6.13: The subimage contains ROI when the sample moves 4 mm to the right.

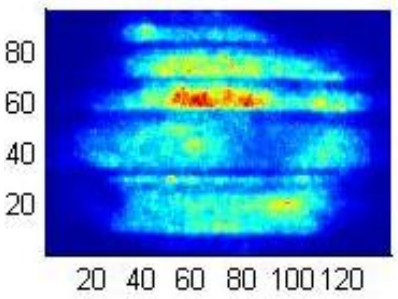

Figure 6.14: The subimage contains ROI when the sample moves 6 mm to the left.

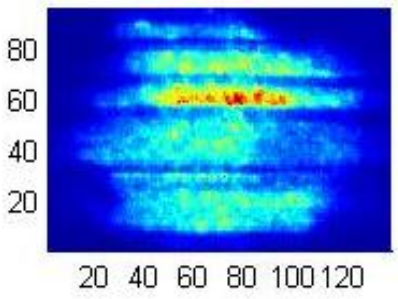

Figure 6.15: The subimage contains ROI when the sample moves 6 mm to the right.

The table 2 shows the computed movement of 4 marks of the ROI in x direction (Δx in pixel) when the sample moves 2-, 4- and 6 mm to the left and to the right.

2 mm to the left	2mm to the right	4 mm to the left	4 mm to the right	6 mm to the left	6 mm to the right
-14	13	-28	26	-44	38
-14	13	-28	26	-44	38
-14	13	-28	26	-44	38
-14	13	-28	26	-44	38

Table 2: The computed movement in x direction of 4 marks of the ROI (Δx in pixel) when the sample moves 2-, 4- and 6 mm to the left and to the right.

The ruler was used to calibrate the movement. Movement of 1mm is corresponding to movement of 7.18 pixels. So the computed movement in x direction of the ROI (Δx in pixel) in the table 2 is transfered to mm when the sample moves 2-, 4- and 6 mm to the left and to the right as be shown in table 3.

2 mm to the left	2mm to the right	4 mm to the left	4 mm to the right	6 mm to the left	6 mm to the right
-1.95	1.81	-3.90	3.62	-6.13	5.29
-1.95	1.81	-3.90	3.62	-6.13	5.29
-1.95	1.81	-3.90	3.62	-6.13	5.29
-1.95	1.81	-3.90	3.62	-6.13	5.29

Table 3: The computed movement in x direction of 4 marks of the ROI (in mm) when the sample moves 2-, 4- and 6 mm to the left and to the right.

The table 4 shows the computed movement of the ROI in x direction (Δx in mm) when the sample moves 2-, 4-,and 6 mm to the left and to the right.

Computed movement of ROI/ mm	Sample movement/ mm
-6.13	-6 (6 mm to the left)
-3,98	-4 (4 mm to the left)
-1.95	-2 (2 mm to the left)
1.81	2 (2 mm to the right)
3.62	4 (4 mm to the right)
5.29	6 (6mm to the right)

Table 4: The computed movement in x direction of the ROI (Δx in mm) when the sample moves 2-, 4- and 6 mm to the left and to the right.

The correlation between the movement of the sample and the computed movement of ROI is illustrated in figure 6.16.

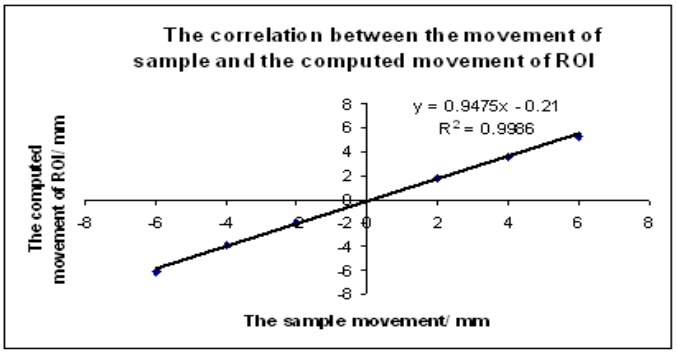

Figure 6.16: The correlation between the movement of the sample and the computed movement of ROI .

6.1.2 Random movement of the sample

The program can follow ROI and find four marks on the mask even if the sample has moved randomly. As can be seen in figures 6.17, and 6.18, four marks which mark ROI (in red colour) are found when the sample moves randomly.

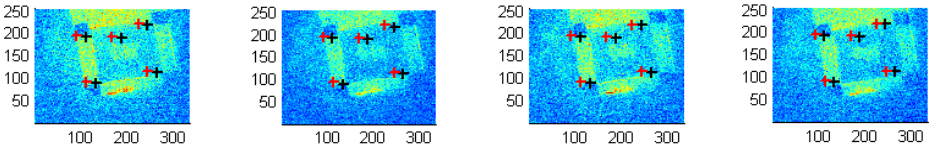

Figure 6.17: The images when the sample has moved randomly.

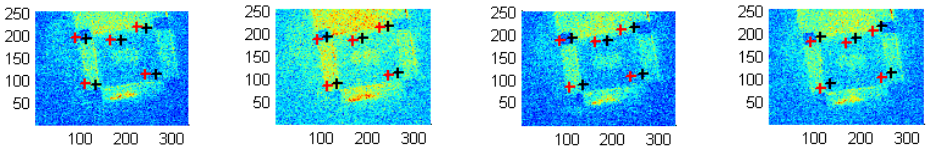

Figure 6.18: The images when the sample has moved randomly.

One of four marks in each image was followed when the sample moved randomly. The illustration of these movements is shown as different colour points, purple, yellow, red, green,blue and black in figure 6.19. It can tell how much the computed movements are when the sample has moved randomly during the time the images were taken.

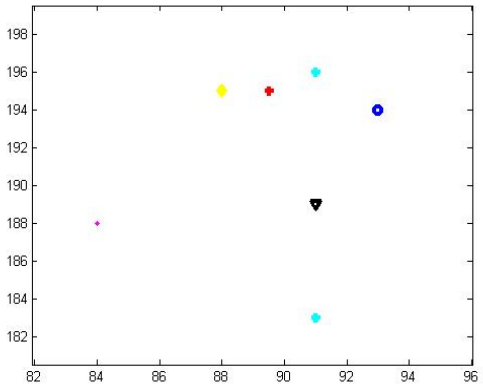

Figure 6.19: The illustration of the marks movement when the sample moved randomly.

The program can extract subimages which contain the same ROI (as can be seen in figures 6.20, and 6.21) even if the sample has moved randomly.

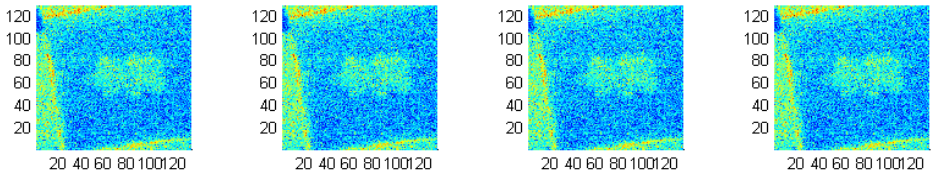

Figure 6.20: The subimage contains ROI when the sample moves randomly.

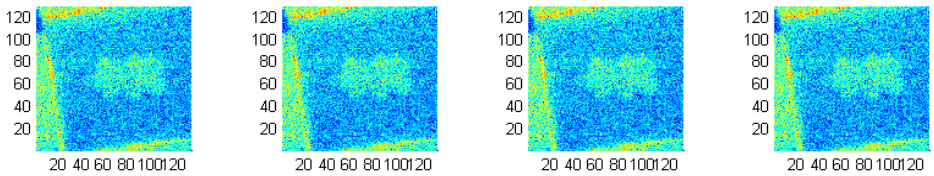

Figure 6.21: The subimage contains ROI when the sample moves randomly.

6.2 Clinical investigation of fluorescence imaging during photodynamic therapy

The images of the tumor on patient were taken in different wavelength bands. The mask was taken in wavelength of 500 nm. Four marks on the mask were visible as be seen in figure 6.22. The tumour was located by this mask.

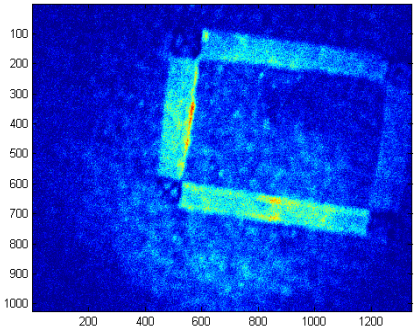

Figure 6.22: The image of the mask on patient.

The evaluated program can find four marks on the mask in different images which were taken in different wavelengths as be shown in figure 6.23.

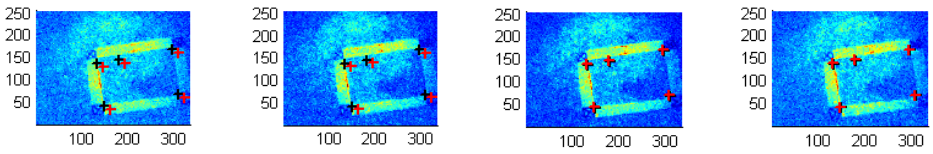

Figure 6.23: The images on patient in different wavelengths of 640 nm, 650 nm, 660 nm and 720 nm from left to right.

The program can also extract the subimages which contain tumor as can be seen in figure 6.24.

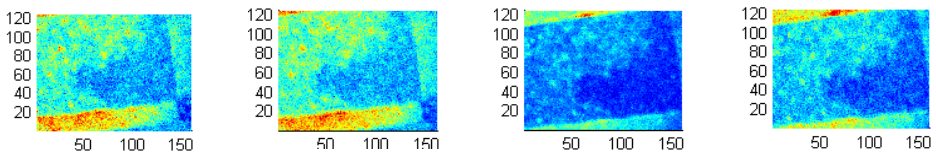

Figure 6.24: The subimages contain the tumor in different wavelengths of 640 nm, 650 nm, 660 nm and 720 nm from left to right.

Four marks in each image were followed when the images were taken in different wavelengths is shown in figure 6.25. Blue, green, pink colors present for four marks in different wavelengths. It can tell how much the computed movements as well as patient movements are.

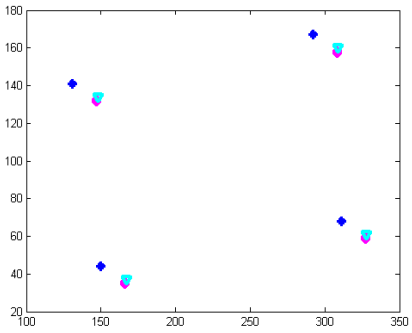

Figure 6.25: The illustration of four marks on the mask when the images were taken in different wavelengths.

Chapter 7

Discussions

7.1 Tracking without mask

The images on patients were taken without mask, as can be seen in figures 7.1, 7.2 and 7.3. The ROI was moving and changing in size in different time when the images were taken. In this case, it is less accurate to delineate the ROI for the clinical treatment. Therefore it is useful to use the mask to localize the ROI.

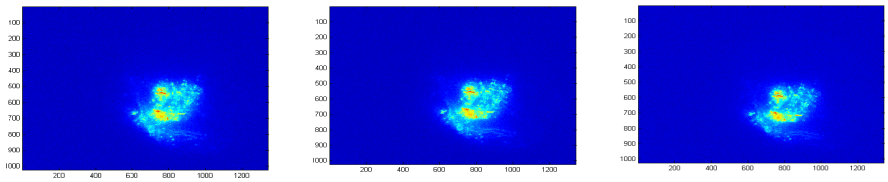

Figure 7.1: The illustration of ROI images on patients without mask.

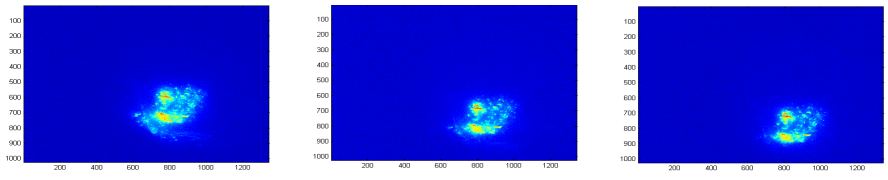

Figure 7.2: The illustration of ROI images on patients without mask.

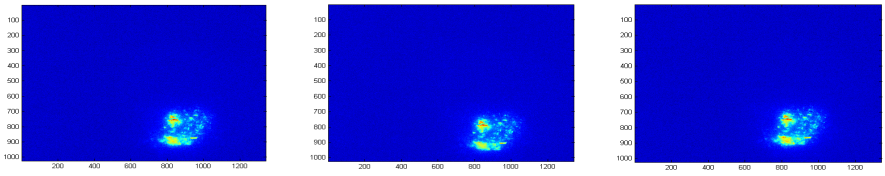

Figure 7.3: The illustration of ROI images on patients without mask.

7.2 Movement of target

The computed movements are shown when the sample moves 2, -4, -6 mm to the left and to the right. As can be seen in figures 6.3, 6.4, 6.5, 6.6, 6.7 and 6.8, when the sample moves 2, -4, -6 mm to the left, the crosses which mark the ROI move to the right and vice versa. It is agreeable to the optical phenomenon. The illustration of the movements is shown in figure 6.9. The correlation between the movement of the sample and the computed movements of the crosses is linear relation as can be shown in figure 6.16.

When the sample moves randomly, the computed movements of the crosses (in red colour) are shown in figures 6.12 and 6.13. The illustration of these computed movements is in figure 6.14. There are 8 images are choosen to be investigated for the computed movements when the sample has moved randomly as be shown in figures 6.17 and 6.18, but there are only 7 points which are illustratted for these computed movements as can be seen in figure 6.19. It can be explained because two moving positions of the sample are coincident.

The extracted subimages which contain the ROI are the same even if the sample has moved 2, -4, -6 mm to the left, to the right as can be seen in figures 6.10, 6.11, 6.12, 6.13, 6.14 and 6.15 or randomly as can be seen in 6.20 and 6.21.

The target should be moved within limit of the light spot (which is created when the light illuminates to the sample) so that the crosses which mark ROI are visible on the images.

The images of tumor on patient were taken on clinic. Four marks on the mask were visible. It is good for the program to find and extract subimages which contain the tumor. As can be seen in figure 6.25, blue, green, pink colors which present for four marks which localize tumor are closed to each other. It means that the patient did not move much during imaging time.

7.3 Mask design

The suitable masks were made. The size of the masks is big enough to cover the ROI/tumour. They were constructed of transparent papers which avoid from fluoresce. The mask with the red marks, x-shape was the best use for the experimental images because the red crosses on the mask are visible in the wavelength of 365 nm.

On the clinic work, the masks were also made of transparent papers, four crosses of x-shape, but blue colour of four crosses was choosen instead of red in experiment. The reason because the light used in PDT was blue laser light with wavelength of 405 nm. In this wavelength, crosses in blue colour were visible.

7.4 Surface roughness

The surface of the skin effects on taking images. It easier to tape the mask on the flat surface of the skin. If the surface is rough, the mask has to be bent when it is taped to cover the tumor. Surface roughness is also difficult for the light spreads over the mask.

Chapter 8

Summary and Conclusions

The skin cancer is the most common of all cancers. It can be treated if it is caught in early stage. It is important to learn which kind of skin cancer is and how to identify it. Fluorescence imaging and photodynamic therapy are conventional therapy to identify and to cure of skin cancer.

This Master's thesis has demonstrated that the design of the template/mask and the evaluated program which can follow the image patern are important. The template covers the ROI/tumor which is moved and dimininished during and between image acquisitions in fluorescence imaging.

Several images were taken to proved the program functions. In the experiment tests, when the sample moves 2, -4, -6 mm to the left, to the right, or randomly, the evaluated program has ability to find the template marks automatically in each image and to extract the same subimages which contain the ROI.

The template was useful on the clinic during fluorescence imaging of skin cancer. The sizes of the templates were big enough to cover the tumors. They were taped on patient's tumors. The multispectral fluorescence imaging system was handled to take the images of tumors (with the templates on). The evaluated program also worked well to find the marks on template and to extract ROI (which contains tumor).

Chapter 9

Future tasks

The future tasks could be the studying of fluorescence bleaching grade in tumor and normal skin and taking images after the PDT treatment.

Chapter 10

Acknowledgement

Bibliography

[1] Jenny svensson. *Fluorescence spectroscopy in tissue for identification and temperature control of embedded lesions* May 2005. Licentiate Thesis. Department of Physics, Lund Institute of technology,Sweden.

[2] Skin cancer. http://adam.about.com (2006-11-10)

[3] http://dermatology.jwatch.org (2006-11-10)

[4] Marica B.Ericson. *Spectroscopic Measurements and Fluorescence Imaging for Treatment and Diagnosis of Skin Cancer* 2004. Doctoral Thesis. Department of Experimental Physics, Chamers University of Technology Gterborg University,Sweden.

[5] http://wwww.shorelaser.com/skincancer.html (2006-11-10).

[6] http://skincancer.dermis.net (2006-11-10).

[7] Effects of Sun on the Skin http://dermatology.about.com/cs/beauty/a/suneffect.htm (2007-01-22).

[8] Pain caused by photodynamic therapy of skin cancer. http://www.blackwell-synergy.com (2006-08-31).

[9] Stefan Andersson-Engels, Claes af klinteberg, K Svanberg and S Svanberg. *In vivo fluorescence imaging for tissue diagnostics* Phys. Med. Biol. *1997, Vol.42,p 815-824*.

[10] http://www-atom.fysik.lth.se/MedOpt/ (2007-03-22)

[11] Ingrid Wang. *Photodynamic Therapy and Laser-Based Diagnostic Studies of Malignant Tumors* 1999. Doctoral Thesis. Department of Physics, Lund University,Sweden.

[12] Nurgul Kmerik. *A novel approach to cancer treatment: Photodynamic therapy* Turkish Journal of Cancer. *2002,Vol.32,no.3*.

[13] Stefan Andersson-Engels . *Laser-induced Fluorescence for Medical Diagnostics* 1989. Doctoral Thesis. Department of Atomic Physics, Lund University,Sweden.

[14] Daniell M.D., J.S.Hill. *A history of photodynamic therapy*, Aust.N.Z.J.Surg.61:340-348. Find this article online.

[15] Spikes J.D. *The historical development of ideas on applications of photosensitised reactions in health sciences. In Pimary photoprocesses in Biology and Medicine 1985, pp.209-227*, Plenum Press,New York.

[16] The History of Photodetection and Photodynamic Therapy. http://www.bioone.org

[17] Chu Dinh Thuy. *Laser for photodynamic therapy*. Institute of Physics and Electronics- VAST Vietnam.

[18] T.J.Vogl et al. *Interstitial photodynamic laser therapy in interventional oncology,* European Radiology, 2004 6 Feb.

[19] Claes af Klinteberg. *On the use of light for the characterization and treatment of malignant tumours* 1999. Doctoral Thesis. Department of Atomic Physics, Lund University,Sweden.

[20] J.Wett et al. *Fluorescence detection of superficical skin cancers* Journal of modern optics, 2000,*Vol. 47, No. 11,pp 2021-2027*

[21] Jacqueline et al. *The application of a compact multispectral imaging system with intergrated excitation source to in vivo monitoring of fluorescence during topical photodynamic therapy of superficial skin cancer* American Society for Photobiology Journal, *Vol. 73, No. 3,pp. 278-282*

[22] A.Johanson, J.Hjelm, E.Ericsson, and S. Andersson-Engels. *Pre-treatment dosimetry for interstitial photodynamic therapy* 2005.

[23] Even Angell-Persen et al. *Influence of light fluence rate on the effects of photodynamic therapy in an orthotropic rat glioma model,* J Neurosury, 2005,*Vol 104,pp 109-117*.

[24] Jablonski Diagram http://www.shsu.edu/.../JABLONSKI.html (2006-12-07).

[25] S.Andersson-Engels and B.C Wilson. *In vivo fluorescence in clinical oncology:fundamental and practical issues*, J.Cell Pharmacol,1992, *Vol 3,pp 48-61*.

[26] S.Andersson-Engels, K.Svanberg, S.Svanberg. *Fluorescence Imaging in Medical Diagnostics*.

[27] Stefan Andersson-Engels, Claes af Klinteberg, K Svanberg, and S Svanberg. *In vivo fluorescence imaging for tissue diagnostics*, Phys.Med.Biol, 1997 *Vol 42, pp 815-824*, UK.

[28] M.L.Henrries, S.Lam, C.MacAulay, J.Qu and B.Palcic. *Diagnostic imaging of the larynx: autofluorescence of laryngeal tumours using the helium-cadmium laser*, J.Laryngol,1995,*Otol.109,pp 108-110*.

[29] B.Kulapaditharom and V.Boonkitticharoen. *Laser-induced fluorescence imaging in localization of head and neck cancers*, Ann.Otol.Rhinol.Laryngol, 1998, *Vol 107, pp 241-246*.

[30] S. Andersson-Engels, J.Johansson, K. Svanberg and S. Svanberg. *Fluorescence imaging and point measurements of tissue: application to the demarcation of malignant tumors and atherosclerotic lesions from normal tissue*. Photochem. Photobiol, 53(6): 807-14, 1991.

[31] J.C Kenedy, R.H. Pottier, and D.C.Pross. *Photodynamic therapy with endogenous protoporphyrin IX: Basic principles and present clinical experience*. J. Photochem. Photobiol. B-Biol, 6(1-2): 143-8, 1990.